Article ID:0253-2778(2016)12-1007-08

Investigation on morphology control of the nanoporous nickel phosphate

NIE Shibin[1], DONG Xiang[1], ZHANG Chi[1], ZHOU Can[1], HU Yuan[2]

(1. *Key Laboratory of Safe and Effective Coal Mining of Ministry of Education, School of Energy Resources and Safety, Anhui University of Science and Technology, Huainan* 232001, *China*;
2. *State Key Laboratory of Fire Science, University of Science and Technology of China, Hefei* 230026, *China*)

Abstract: VSB-1 was synthesized by hydrothermal method in various synthesis conditions, and the influences of the synthesis conditions on the morphology of VSB-1 were studied. The results show that by adjusting the synthesis conditions, different morphologies of VSB-1 can be obtained. The morphology of VSB-1 changes from a needle-like to mushroom-like shape and the diameter of the VSB-1 also varies. The morphologies influence the surface areas of VSB-1. The needle-like VSB-1 has a higher BET (Brunauer-Emmet-Teller) surface than that of mushroom-like VSB-1. Meanwhile, the results show that VSB-1 has high thermal stability.

Key words: nanoporous nickel phosphate; morphology; VSB-1; hydrothermal method

CLC number: X932; O611.4 **Document code**: A doi: 10.3969/j.issn.0253-2778.2016.12.007

Citation: NIE Shibin, DONG Xiang, ZHANG Chi, et al. Investigation on morphology control of the nanoporous nickel phosphate[J]. Journal of University of Science and Technology of China, 2016, 46(12): 1007-1014.

多孔磷酸镍形貌控制研究

聂士斌[1],董 翔[1],张 驰[1],周 灿[1],胡 源[2]

(1. 煤矿安全高效开采省部共建教育部重点实验室,安徽理工大学能源与安全学院,安徽淮南 232001;
2. 中国科学技术大学火灾科学国家重点实验室,安徽合肥 230026)

摘要:利用水热合成法制备了 VSB-1,并研究了不同合成条件对 VSB-1 形貌的影响. 研究表明,通过调节合成条件可以制备不同形貌的 VSB-1. VSB-1 的形貌可以从针状变成蘑菇状,并且 VSB-1 颗粒尺寸以及比表面积也发生了变化. 针状 VSB-1 相比蘑菇状 VSB-1 具有更高的比表面积. 同时研究表明,VSB-1 具有较好的高温热稳定性,在 400 ℃仍能保持蘑菇状形貌.

关键词:多孔磷酸镍;形貌;VSB-1;水热合成法

Received: 2016-04-12; **Revised**: 2016-07-22

Foundation item: Supported by National Natural Science Foundation of China (51303004, U1332134), PhD Programs Foundation of Ministry of Education of China (20133415120001).

Biography: NIE Shibin (corresponding author), male, born in 1983, PhD/associate professor. Research field: flame retardant polymer composites. E-mail: nsb@mail.ustc.edu.cn

0 Introduction

Zeolite molecular sieves have been attracting wide attention due to their unique internal structure that can be used in many fields. The aluminosilicate zeolites, as an important kind of zeolites, have represented the predominant class of microporous materials for a long time[1]. Porous phosphates containing a transition metal are becoming more and more promising. Transition metals can be used as structure-directing agents in the synthesis of porous phosphates. Meanwhile, some novel properties not seen in traditional aluminosilicate zeolites can be realized with the introduction of transition elements[2-4]. Guillou et al. successively synthesized nanoporous nickel phosphates molecular sieves-VSB-1[5]. The structure of VSB-1 is based on a large unidimensional channel composed of 24 NiO_6 and 12 P—OH groups in each window of channel. The typical preparation has been achieved by hydrothermal synthesis at 180 ℃ for 5 d in the presence of organic diamines as templates or structure-directing agents[5]. VSB-1 has shown excellent properties such as hydrogen storage[4], selective hydrogenation[6] and so on[7]. Furthermore it can be used as a synergist in intumescent flame retardancy system[8-9].

Because the morphology of nanoporous nickel phosphate has a close relationship with its properties, the crystal shape and size are necessary for their applications. The strategy to control the crystal shape and size is getting more and more attention. There have been some reports about molecular sieves controlling surface morphology[10-12]. However, as a promising catalyst, the controlling surface morphology of VSB-1 still lacks investigation.

So in this work, based on the classical way to synthesize VSB-1, VSB-1 was synthesized by hydrothermal method in various conditions. The influence of the pH value, reactant time and ratio of reactant compositions on the morphology of the final products were studied, respectively.

1 Experimental

1.1 Materials

Nickel (Ⅱ) dichloride hexahydrate (mass fraction 98%), and phosphoric acid (mass fraction 85%) were purchased from Sinopharm Chemical Reagent Co., Ltd. Ammonia was obtained from Shanghai Yuanda Petoxide Co., Ltd.

1.2 The synthesis of nanoporous nickel phosphates VSB-1

Typical synthetic steps were as follows: Firstly, nickel the source was dissolved in deionized water, followed by adding phosphoric acid. Then, after fully mixed, the nickel dichloride aqueous solution was added with ammonium fluoride. Then proper amount of aqueous ammonia was subsequently dropped into the aqueous solution with gentle agitation to adjust pH. The resulting green solution was aged for half an hour and then heated in 100 mL Teflon lined reactors at 180 ℃. The synthesis conditions are summarized in Tabs. 1～3. After that, the yellowish green powders taken out from the autoclaves were filtered and washed with deionized water at room temperature, and then dried in an oven at 100 ℃ in air condition overnight.

1.3 Characterization

X-ray diffraction (XRD) patterns were performed using a Japan Shimadzu XRD-6000 X-ray diffractometer equipped with graphite monochromatized high-intensity Cu-Ka radiation (λ=0.154 2 nm), and operated at 40 kV voltage and 30 mA current.

The scanning electron microscopy (SEM) images were taken using KYKY-2800B (produced by KYKY Technology Co., Ltd., China) and Sirion200 scanning electron microscopes (produced by FEI, USA). The char was adhibitted on the copperplate, and then coated with gold/palladium alloy ready for imaging.

Tab. 1 Effect of the composition in the synthesis of VSB-1

sample	synthesis conditions						
	$NiCl_2 \cdot 6H_2O$	H_3PO_4	NH_4F	H_2O	pH	temperature/℃	reaction time/h
NP-0	1	1	0	40	2.5	180	72
NP-1	1	1	1	40	2.5	180	72
NP-2	1	1.5	1	40	2.5	180	72
NP-3	1	2	1	40	2.5	180	72
NP-4	1	3	1	40	2.5	180	72
NP-5	1	1	1.5	40	2.5	180	72
NP-6	1	1	2	40	2.5	180	72
NP-7	1	1	3	40	2.5	180	72

Tab. 2 Effect of the pH in the synthesis of VSB-1

sample	synthesis conditions						
	$NiCl_2 \cdot 6H_2O$	H_3PO_4	NH_4F	H_2O	pH	temperature/℃	reaction time/h
NP-8	1	1	1	40	1.5	180	72
NP-9	1	1	1	40	3.5	180	72
NP-10	1	1	1	40	5.5	180	72

Tab. 3 Effect of the reaction time in the synthesis of VSB-1

sample	synthesis conditions						
	$NiCl_2 \cdot 6H_2O$	H_3PO_4	NH_4F	H_2O	pH	temperature/℃	reaction time/h
NP-11	1	1	1	40	2.5	180	24
NP-12	1	1	1	40	2.5	180	48
NP-13	1	1	1	40	2.5	180	96
NP-14	1	1	1	40	2.5	180	120

Thermogravimetric analysis (TGA) was performed on a Mettler-Toledo TGA/SDTA851e instrument with a heating rate of 20 ℃ · min^{-1} and air flow rate of 50 mL · min^{-1}. Samples were measured in an alumina crucible with a mass of about 5 mg.

The BET (Brunauer-Emmet-Teller) surface area and pore structure were analyzed using JW-BK222 specific surface area analyzer produced by JWGB SCI. & TECH. Each sample was heat-treated at 623 K for 1 h before measurement.

2 Results and discussion

2.1 Effect of the reactant compositions in the synthesis of VSB-1

Changing reactant compositions, the diameter and morphology of VSB-1 could be both controlled.

By the series of experiments represented in Tab. 1, the effect of the phosphoric acid and ammonium fluoride on synthesis and morphology controlling of VSB-1 is discussed. Fig. 1 shows the XRD results of samples NP-1 to NP-4. The diffraction peak positions of NP-1 to NP-3 patterns agree well with that of VSB-1 obtained by previous literature[5,17], which indicates the amount of molar ratio of H_3PO_4 : $NiCl_2$ from 1 : 1 to 2 : 1

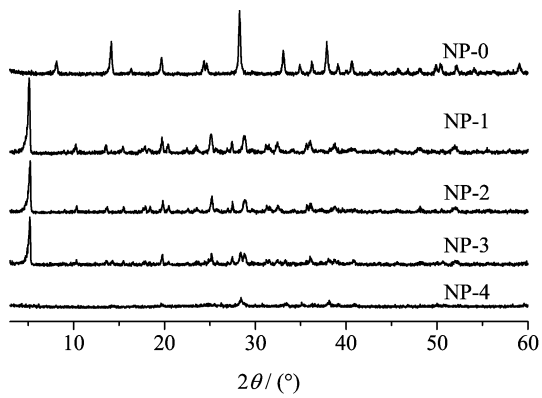

Fig. 1 The XRD patterns of samples NP-0 to NP-4

(under the same other conditions) can lead to successful crystallization of VSB-1. Whereas, once the ratio of H_3PO_4 : $NiCl_2$ increase to 3 : 1, the structure of VSB-1 can not be formed (NP-4). Meanwhile, fluorid ion is very important to the synthesis of VSB-1. The XRD patterns shown in Fig. 2 confirm that the molar ratio of reactant mixtures $NiCl_2 \cdot 6H_2O$: H_3PO_4 : NH_4F : H_2O = 1 : 1 : 0 : 40 at the reaction temperature 180 ℃ for 72 h with pH 2.5 fails to synthesize VSB-1, forming a kind of nickel hydrogen phosphite hydroxide. VSB-1 can be excellently formed with the molar ratio of NH_4F : $NiCl_2$ from 1 : 1 to 3 : 1.

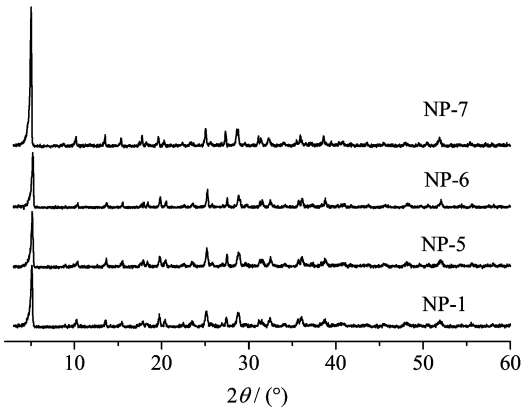

Fig. 2 The XRD patterns of samples NP-5 to NP-7

Fig. 3 shows the morphologies of VSB-1 from NP-1 to NP-4. As to NP-1, the particles present a mushroom-like morphology with a diameter of about 30 μm formed by the sharp needle-like structure. Only by changing the molar ratio of H_3PO_4 : $NiCl_2$ to 1.0～2.0 : 1 and keeping NH_4F : $NiCl_2$ unchanged, can the morphology of VSB-1 change. With H_3PO_4 : $NiCl_2$ equal to 1.5 : 1, NiP-2 has a number of morphologies, such as needle-like shape, partly mushroom-like shape and mushroom-like shape. With H_3PO_4 : $NiCl_2$ equal to 2 : 1, mushroom-like morphology (NP-3) disappears. NP-4 (H_3PO_4 : $NiCl_2$ equal to 3 : 1) has a tomato-like morphology which is quite

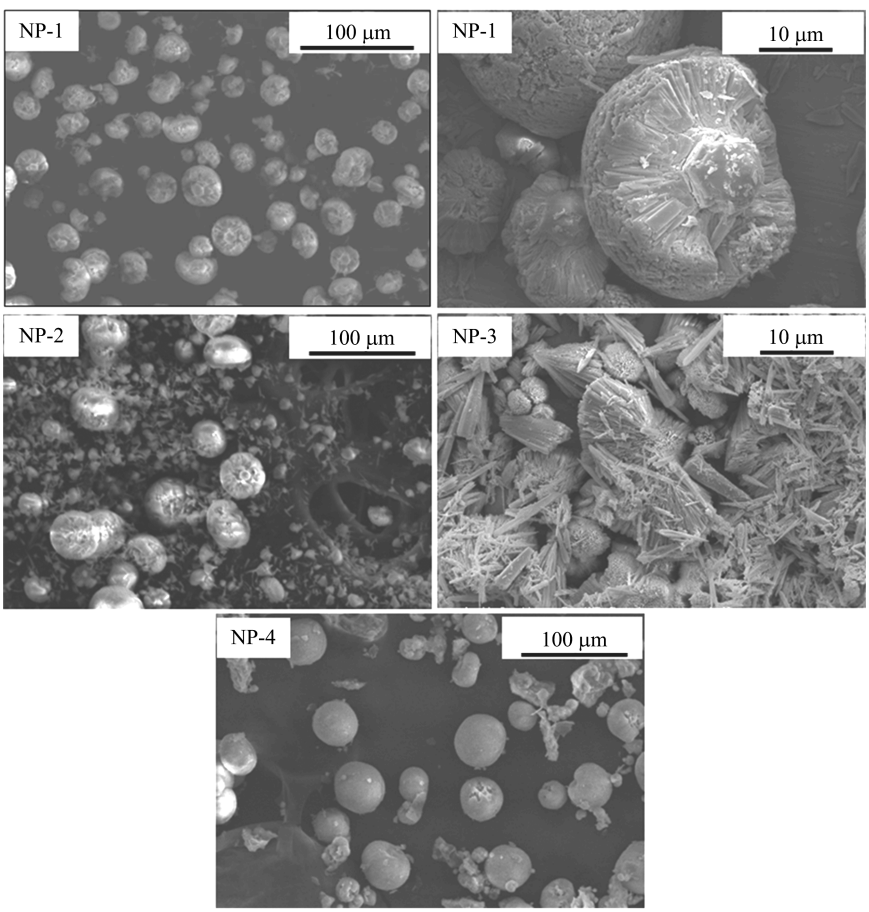

Fig. 3 The morphologies from NP-1 to NP-4

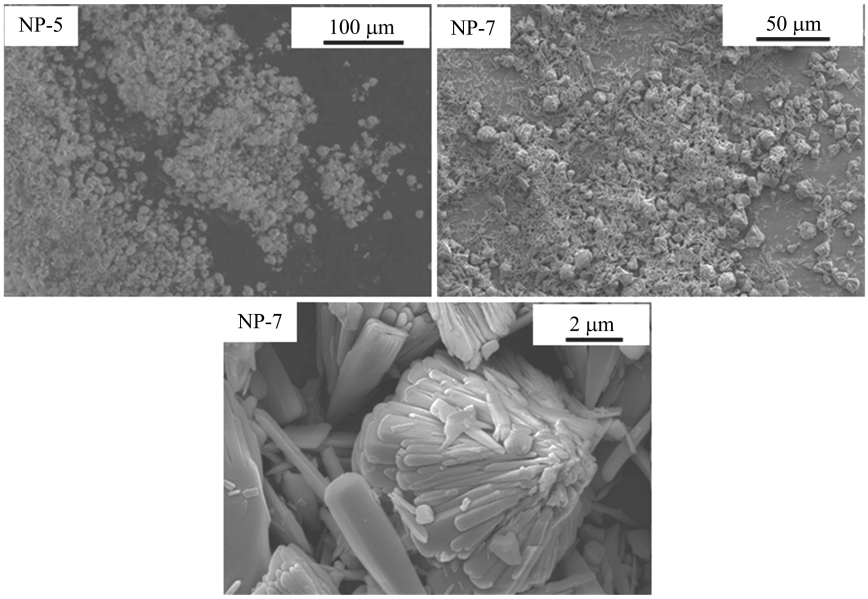

Fig. 4 The morphologies of NP-5 and NP-7

different from others due to the failure of the formation of VSB-1 structure. Fig. 4 shows the particle morphologies of NP-5 and NP-7. The particle diameter of NP-5 with NH_4F : $NiCl_2$ equal to 1.5 : 1 reduces to about 15 μm showing mainly partly mushroom-like shape. Once NH_4F : $NiCl_2$ reaches to 3 : 1 (NP-7), the particle morphology is still mainly partly mushroom-like shape, and the mushroom-like particles present different diameter range. It is obvious that the composition ratio affects the crystal procedure of samples. By changing composition ratio, the diameter and morphology of VSB-1 could both be controlled.

2.2 Effect of pH values in the synthesis of VSB-1

pH values of the reactant solution have a signal effect on the crystal procedure of VSB-1.

The pH value is also a crucial factor in the process of crystallization of porous structure material. By the series of experiments represented in Tab. 2, the effect of pH values is discussed. Fig. 5 shows the XRD results of samples synthesized by different pH values. As can be seen in Fig. 5, fine VSB-1 structure can be obtained at pH 1.5, 2.5 and 3.5. The phase of NP-10 is determined as a kind of ammonium nickel phosphate hydrate by searching the powder diffraction file database, showing that VSB-1 can not be obtained with the pH as high as 5.5. The SEM images (Fig. 6) indicate that pH of the reactant solution has a signally effect on the crystal procedure. Compared with mushroom-like particles with 30 μm (NP-1), which are attained under pH 2.5, the NP-8 and NP-9 exhibit quite different morphologies. A mass of needle-like shape particles constitute NP-8, revealing that the final product may stay at the initial stage of the crystallization procedure when pH is 1.5. NP-9 shows disorderly morphologies at pH 3.5, showing lower morphology regularity compared with those obtained at pH 1.5 and 2.5.

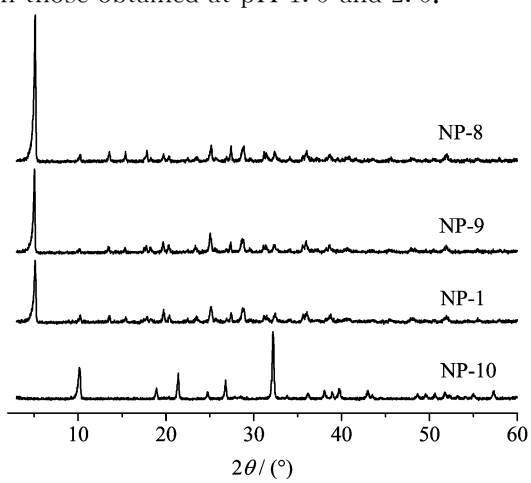

Fig. 5 The XRD patterns of VSB-1 at different pH values

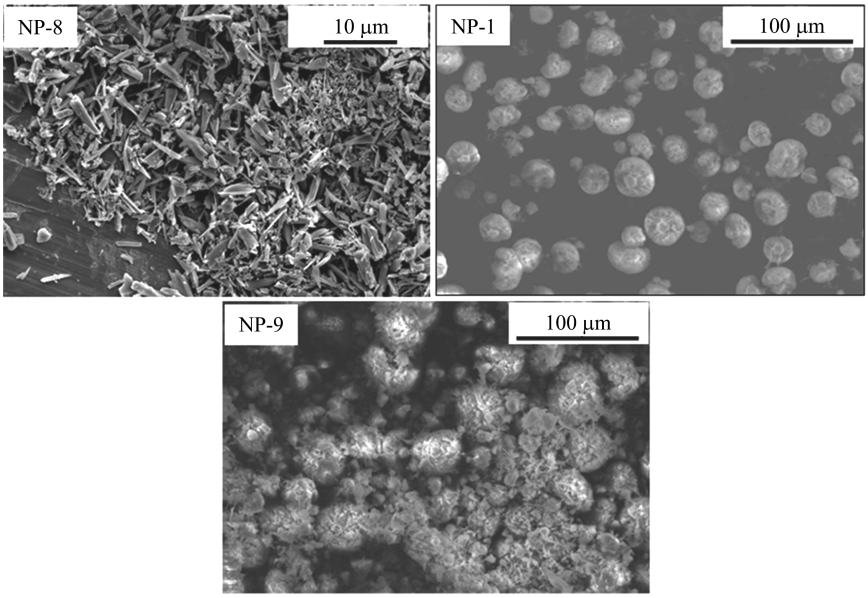

Fig. 6 The SEM images of VSB-1 at different pH

2.3 Effect of the reaction time in the synthesis of VSB-1

VSB-1 is more fully crystallized when the reaction time prolongs and the diameter of particles becomes greater.

Effect of the reaction time on the synthesis of VSB-1 is shown in Tab. 3. Keeping the molar ratio of reactant composition $NiCl_2 \cdot 6H_2O : H_3PO_4 : NH_4F : H_2O = 1 : 1 : 1 : 40$ and the pH 2.5 unchanging, different reaction times in a wide range from 1 to 5 d have been tried. Fig. 7 shows the XRD results of VSB-1 synthesized by different reaction times.

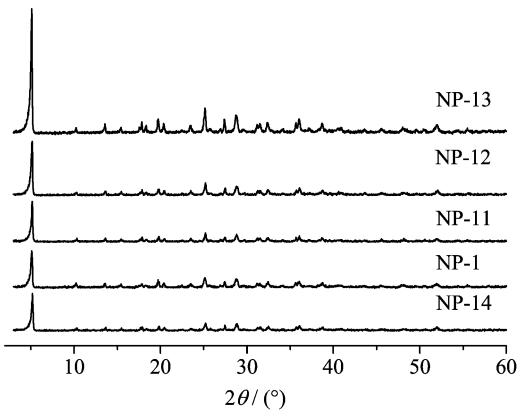

Fig. 7 The XRD patterns of VSB-1 synthesized with different reaction times

It can be observed that the VSB-1 is more fully crystallized with the reaction time being prolonged, as is confirmed by the SEM images (Fig. 8). As shown in Fig. 8, VSB-1 shows mixed morphologies with both needle-like shape and mushroom-like shape when the reaction time is shorter than 72 h. Once the reaction time is as long as 72 h, there is only mushroom-like shape. Moreover, the diameter of particles becomes greater as the reaction time prolongs above 72 h.

2.4 Thermal stability and BET surface investigation on synthesized VSB-1

A selection of mushroom-like VSB-1 (NP-1) and needle-like VSB-1 (NP-8) was used to study the thermal stability and BET properties of VSB-1 with different morphologies. The BET surface areas of NP-1 and NP-8 were determined by N_2 adsorption. The BET surface areas of NP-1 and NP-8 are 110.6 $m^2 \cdot g^{-1}$ and 144.1 $m^2 \cdot g^{-1}$, respectively. The average adsorption pore sizes for NP-1 and NP-8 were 2.48 nm and 2.83 nm, respectively. The results of BET are consistent with the results of SEM. The mushroom-like shape is formed the needle-like structure, so NP-1 has a lower BET surface area compared with that of NP-8. The morphology of VSB-1 (NP-8) heated at 400 ℃ is shown in Fig. 9. It can be observed that NP-8 still keeps the mushroom-like shape.

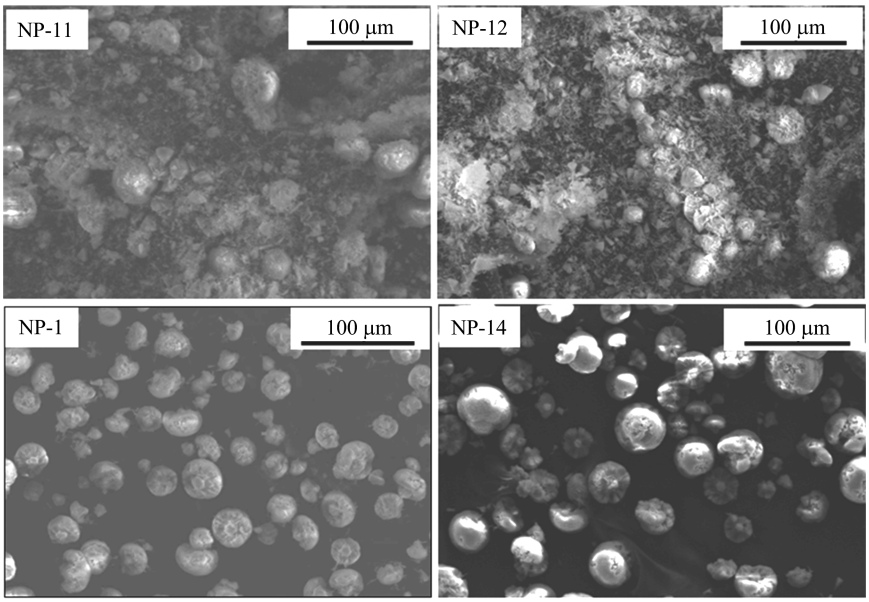

Fig. 8 The morphologies of VSB-1 synthesized with different reaction times

The morphology of VSB-1 does not change even at 400 ℃, which shows that VSB-1 has a good thermal stability.

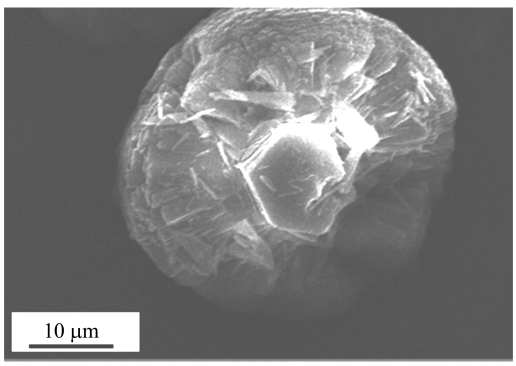

Fig. 9 The morphology of NP-8 heated at 400 ℃

3 Conclusion

The different morphologies of nanoporous nickel phosphate-VSB-1 were synthesized by the hydrothermal method under various synthesis conditions. The results show that by adjusting the synthesis conditions such as pH value, reaction time, reaction temperature and ratio of reactant compositions, different morphologies of VSB-1 can be obtained. The morphology of VSB-1 changes from needle-like to mushroom-like shape, and the diameter of the VSB-1 also varies. The morphologies influence the surface areas of VSB-1. The needle-like VSB-1 has a higher BET surface than that of mushroom-like VSB-1. The VSB-1 shows high thermal stability, and the mushroom like shape of VSB-1 can be kept even at 400 ℃. The morphology does not greatly influence the thermal behaviour of VSB-1.

References

[1] FÉREY G, CHEETHAM A K. Prospects for giant pores[J]. Science, 1999, 283(5405): 1 125-1 126.

[2] LIN R H, DING Y J. A review on the synthesis and applications of mesostructured transition metal phosphates[J]. Materials, 2013, 6(1): 217-243.

[3] CHEETHAM A K, FÉREY G, LOISEAU T. Open-framework inorganic materials [J]. Angewandte Chemie International Edition, 1999, 38(22): 3 268-3 292.

[4] FORSTER P M, ECKERT J, CHANG J S, et al. Hydrogen adsorption in nanoporous nickel (II) phosphates [J]. Journal of the American Chemical Society, 2003, 125(5): 1 309-1 312.

[5] GUILLOU N, GAO Q M, NOGUES M, et al. Zeolitic and magnetic properties of a 24-membered ring porousnickel (ll) phosphate, VSB-1 [J]. Comptes Rendus de l'Académie des Sciences-Series II C - Chemistry, 1999, 2(7/8): 387-392.

[6] CHANG J S, PARK S E, GAO Q M, et al. Catalytic conversion of butadiene to ethylbenzene over the nanoporous nickel(II) phosphate, VSB-1[J]. Chemical

Communications,2001, 9(9): 859-860.
[7] TIMOFEEVA M N, PANCHENKO V N, HASAN Z, et al. Catalytic potential of the wonderful chameleons: Nickel phosphate molecular sieves[J]. Applied Catalysis A: General,2013, 455: 71-85.
[8] NIE S B, ZHANG C, PENG C, et al. Study of the synergistic effect of nanoporous nickel phosphates on novel intumescent flame retardant polypropylene composites [J]. Journal of Spectroscopy, 2015, 2015:289298.
[9] NIE S B, HU Y, SONG L, et al. Study on a novel and efficient flame retardant synergist-nanoporous nickel phosphates VSB-1 with intumescent flame retardants in polypropylene [J]. Polymers for Advanced Technologies,2008, 19(6): 489-495.
[10] WU H Y, LIU M, TAN W, et al. Effect of ZSM-5 zeolite morphology on the catalytic performance of the alkylation of toluene with methanol[J]. Journal of Energy Chemistry,2014, 23(4): 491-497.
[11] LEE H J, KIM S H, KIM J H, et al. Synthesis and characterization of zeolites MTT and MFI, with controlled morphologies using mixed structure directing agents[J]. Microporous and Mesoporous Materials, 2014, 195: 205-215.
[12] JHUNG S H, YOON J W, HWANG Y K, et al. Morphology control of the nanoporous nickel phosphate VSB-5 from large crystals to nanocrystals [J]. Microporous and Mesoporous Materials, 2006, 89: 9-15.

(上接第992页)

[2] CHEN C, LIU G. Effects of axial guiding magnetic field on microwave power of backward-wave oscillators [J]. High Power Laser and Particle Beams, 2000, 12: 745-748.
[3] CHEN C, LIU G, HUANG W, et al. A repetitive X-band relativistic backward-wave oscillator[J]. IEEE Trans Plasma Sci, 2000, 25: 1 108-1 111.
[4] REN Y, WANG F, CHEN W, et al. Development of a superconducting magnet system for microwave application[J]. IEEE Trans Appl Supercond, 2010, 20(3): 1 912-1 915.
[5] LVOVSKY Y, STAUTNER W, ZHANG T. Novel technologies and configurations of superconducting magnets for MRI[J]. Supercond Sci Technol, 2013, 26(9): 093001.
[6] HIROSE R, KAMIKADO T, OKUI Y, et al. Development of 7 T cryogen-free superconducting magnet for gyrotron[J]. IEEE Trans Appl Supercond, 2008, 12: 920-923.
[7] WANG Q, DAI Y, ZHAO B, et al. Design of superconducting magnet for background magnetic field [J]. IEEE Trans Appl Supercond, 2008, 18(2): 548-551.
[8] CHOI Y S, KIM D L, LEE B S, et al. Conduction-cooled superconducting magnet for material control application[J]. IEEE Trans Appl Supercond, 2009, 19(3): 2 190-2 193.
[9] ZHANG X, REN Y, WANG F, et al. Development of a superconducting magnet system with zero liquid helium boil-off[J]. J Supercond Novel Magn, 2014, 27(4): 1 027-1 030.
[10] YAMASHITA T, NISHIJIMA S, TAKAHATA K, et al. Instability of impregnated windings induced by epoxy cracking[J]. IEEE Trans Magn, 1989, 25(2): 1 524-1 527.
[11] WANG Q, DAI Y, ZHAO B, et al. Development of large-bore superconducting magnet with zero-vapor liquid helium[J]. IEEE Trans Appl Supercond, 2008, 18: 787-790.
[12] CHEN P, DAI Y, WANG Q, et al. Mechanical behavior analysis of a 1 MJ SEMS magnet[J]. IEEE Trans Appl Supercond, 2010, 20(3): 1 916-1 919.